Human Molecular Genetics, 2013, Vol. 22, No. 16 **3315–3328**
doi:10.1093/hmg/ddt192
Advance Access published on May 10, 2013

Nilotinib reverses loss of dopamine neurons and improves motor behavior via autophagic degradation of α-synuclein in Parkinson's disease models

Michaeline L. Hebron†, Irina Lonskaya† and Charbel E.-H. Moussa*

Department of Neuroscience, Laboratory for Dementia and Parkinsonism, Georgetown University Medical Center, Washington, DC 20057, USA

Received March 20, 2013; Revised and Accepted April 22, 2013

Parkinson's disease is a movement disorder characterized by death of dopaminergic substantia nigra (SN) neurons and brain accumulation of α-synuclein. The tyrosine kinase Abl is activated in neurodegeneration. Here, we show that lentiviral expression of α-synuclein in the mouse SN leads to Abl activation (phosphorylation) and lentiviral Abl expression increases α-synuclein levels, in agreement with Abl activation in PD brains. Administration of the tyrosine kinase inhibitor nilotinib decreases Abl activity and ameliorates autophagic clearance of α-synuclein in transgenic and lentiviral gene transfer models. Subcellular fractionation shows accumulation of α-synuclein and hyper-phosphorylated Tau (p-Tau) in autophagic vacuoles in α-synuclein expressing brains, but nilotinib enhances protein deposition into the lysosomes. Nilotinib is used for adult leukemia treatment and it enters the brain within US Food and Drug Administration approved doses, leading to autophagic degradation of α-synuclein, protection of SN neurons and amelioration of motor performance. These data suggest that nilotinib may be a therapeutic strategy to degrade α-synuclein in PD and other α-synucleinopathies.

INTRODUCTION

Parkinson's disease (PD) is a motor disorder characterized by death of dopaminergic (DA) neurons in the substantia nigra (SN) (1–3) and formation of inclusions known as Lewy bodies (LBs) (4–13), which primarily contain aggregated α-synuclein (4,7–9,11,13). Activation via phosphorylation of Abl (Abelson) is detected in neurodegenerative diseases (14–17). Abl is a tyrosine kinase distributed in the nucleus and cytosol and involved in a wide range of functions, including apoptosis (18). Abl levels are increased in the nigrostriatal region of PD patients (14,15), and Abl inhibition enhances survival of DA neurons in PD models (14). Phosphorylated Abl is present in neuronal cell bodies in Alzheimer's disease (16,17,19,20), frontotemporal dementia linked to chromosome-17 and Guam Parkinson-dementia and Pick's disease (19). Activation of Abl in the mouse forebrain induces neurodegeneration in the hippocampus and striatum (21). Therefore, an increase in Abl activity via phosphorylation may be associated with the α-synuclein pathology detected in PD and other α-synucleinopathies, including multiple system atrophy (MSA), as well as progressive supranuclear palsy (PSP) and cortico-basal degeneration.

Normal autophagy is a dynamic multi-step process that includes several compartments referred to as the sequestering phagophore (22), the autophagosome (23), the amphisome (24,25) and the autophagolysosome (23). Changes in normal autophagy and accumulation of autophagic vacuoles (AVs), also known as autophagosomes, are recognized in neurodegeneration, including PD (26–33). Our work and other reports show that α-synuclein accumulation is associated with impairment of autophagy in PD models (33–35). Previous studies show that Abl knockout protects against 1-methyl-4-phenyl-1,2,3,6-tetrahydropyridine toxicity in PD animal models (15). Therefore, Abl inhibition may lead to α-synuclein degradation and provide a therapeutic potential for α-synucleinopathies. Nilotinib is a second-generation Abl inhibitor, was approved by the US Food and Drug Administration (FDA) in 2007, for the treatment (300–400 mg orally twice daily) of adult patients with chronic and accelerated phase (AP) Philadelphia

*To whom correspondence should be addressed at: Department of Neuroscience, Laboratory for Dementia and Parkinsonism, Georgetown University School of Medicine, 3970 Reservoir Rd, NW, TRB, Room WP26B, Washington DC 20057, USA. Tel: +1 2026877328; Fax: +1 2026870617; Email: cem46@georgetown.edu
†I.L. and M.L.H. are co-first authors.

© *The Author 2013. Published by Oxford University Press. All rights reserved.*
For Permissions, please email: journals.permissions@oup.com

Downloaded from https://academic.oup.com/hmg/article/22/16/3315/627350 by guest on 21 August 2022

chromosome-positive (Ph+) chronic myelogenous leukemia (CML) (36–38). The current studies evaluated the effects of Abl inhibition via nilotinib treatment on clearance of α-synuclein in animal models of synucleinopathies. Transgenic α-synuclein mice harboring the arginine to threonine (A53T) mutation of human α-synuclein under the control of prion promoter (39) were used as a model of α-synucleinopathies. Because A53T mice do not express α-synuclein in SN neurons, lentiviral expression of human wild-type α-synuclein in the SN was used to mimic PD pathology and evaluate the effects of nilotinib on α-synuclein accumulation in DA neurons and motor behavior.

RESULTS

Abl activation is associated with accumulation of α-synuclein

To examine the relationship between Abl and α-synuclein, male C57BL/6 mice were stereotaxically injected with 1×10^4 multiplicity of infection (m.o.i.) lentiviral Abl, or α-synuclein (or LacZ) bilaterally into the SN. Lentiviral injection significantly increased α-synuclein (42%) over LacZ level (Fig. 1A and B, first blot, $n = 9$ animals) 6 weeks post-injection. α-Synuclein expression led to an increase in total Abl (110%) relative to actin and tyrosine 412 (T412) phosphorylation (289%) relative to total Abl (Fig. 1A and B, $P < 0.05$, $n = 9$) compared with LacZ expressing mice, indicating Abl activation. Conversely, lentiviral expression of Abl in the mouse SN led to an increase (204%) in total Abl relative to actin (Fig. 1D and E, $P < 0.05$, $n = 9$) and T412 phosphorylation (231%) relative to total Abl and resulted in increased levels of monomeric (51%) and high molecular weight α-synuclein (relative to actin) 6 weeks post-injection compared with LacZ. To verify that both lentiviral LacZ and Abl were expressed, a V5-epitope tag of the lentiviruses was probed with immunohistochemistry (IHC). Staining of 20 μm thick SN sections showed V5 (Fig. 1E) and Abl (Fig. 1F) co-localized (Fig. 1G) in lentiviral-Abl injected brains, while staining of LacZ injected SN showed V5 (Fig. 1H) and endogenous Abl (Fig. 1I) without co-localization (Fig. 1J), indicating that the V5-tagged lentivirus was expressed. To evaluate the relationship between Abl and α-synuclein in the human brain, western blot (WB) was performed on homogenized frozen striatal (caudate) brain tissues (described in 33) from nine sporadic PD patients and seven age-matched control subjects. Human post-mortem PD striatal extracts showed an increase in total Abl (220%) relative to actin and T412 (267%) relative to total Abl (Fig. 2K and L) compared with control subjects ($P < 0.02$, two-tailed t-test), suggesting a relationship between Abl activation and α-synuclein accumulation in PD.

Pharmacological inhibition of Abl was previously demonstrated in response to Aβ fibrils in rat hippocampal neurons, where imatinib mesylate (Gleevec or STI571) or RNAi (40) protected against Aβ toxicity. Despite lack of evidence that Gleevec crosses the blood brain barrier, Abl inhibition with Gleevec was evaluated as a potential strategy to slow neurodegeneration (41). Nilotinib is a second-generation Abl tyrosine kinase inhibitor (TKI) formerly known as AMN107 (36–38). Mass spectroscopy analysis revealed that intraperotenial (i.p.) injection of 10 or 20 mg/kg nilotinib into wild-type mice ($n = 5$ animals/time point) led to detection of up to 30 ng nilotinib (310 nM) per mg brain tissue 3–4 h after injection (Fig. 1M) and nilotinib was still detectable at 3.4 ng/mg (35 nM) 7–8 h post-injection, indicating that nilotinib enters the brain and is washed out after several hours. To determine the biological effects of nilotinib *in vivo*, 2-month-old C57BL6 mice were i.p. injected once a day with 10 mg/kg nilotinib or DMSO (30 μl) for three consecutive weeks, and total brain extracts were analyzed with WB. Chronic nilotinib treatment led to a slight (11%) decrease in total Abl relative to tubulin but T412 Abl was significantly decreased (52%) relative to total Abl compared with DMSO-treated control (Fig. 1N and O, $P < 0.05$, $n = 10$ animals). No changes were detected in T245 Abl relative to actin or total Abl (Fig. 1N, third blot). Additionally, the level of proteins detected with pan phospho-tyrosine antibody was also reduced in nilotinib compared with DMSO-treated animals, suggesting that nilotinib is a non-specific TKI inhibitor. The decrease in total Abl could be due to the chronic treatment and the decrease in tyrosine-phosphorylated proteins.

Nilotinib decreases brain and blood α-synuclein levels

The effects of nilotinib on α-synuclein levels were tested in 7–8-month-old transgenic α-synuclein mice that harbor the A53T mutation of α-synuclein (39). Enzyme-linked immunosorbent assay (ELISA) measurement of A53T mice total brain lysates showed accumulation of up to 885 ng/ml human α-synuclein (Fig. 2A) in 7–8-month-old mice treated with DMSO compared with wild-type control ($P < 0.05$, $n = 10$), but daily i.p. injection of 10 mg/kg nilotinib for 3 weeks significantly decreased α-synuclein to 467 ng/ml ($P < 0.05$, $n = 10$), indicating that once a day treatment with the TKI, nilotinib, decreases brain α-synuclein levels. A significant increase in caspase-3 activity (Fig. 2B, 670%, $P < 0.05$, $n = 64$) was observed in A53T mice brains and nilotinib reversed this increase to 201% compared with wild-type age-matched controls with and without nilotinib ($n = 64$). The effects of lower dose and longer periods of treatment were evaluated in the blood and brain of 5–6-month-old A53T mice, which were injected every other day with 1 or 5 mg/kg nilotinib for 6 weeks (compared with 3 weeks). The whole blood was collected via cardiac puncture and brain tissues were extracted in lysis buffer and analyzed by ELISA. A total of 665 ng/ml human α-synuclein was observed in the brain of A53T treated with DMSO compared with C57BL/6 age-matched control (Fig. 2C, $P < 0.05$, $n = 10$), but α-synuclein levels decreased to 503 ng/ml with 5 mg/kg and 344 ng/ml with 1 mg/kg nilotinib for 6 weeks. A higher concentration of human α-synuclein (1635 ng/ml) was detected in the whole blood of A53T mice treated with DMSO compared with C57BL/6 age-matched control (Fig. 2D, $P < 0.05$, $n = 10$), and, again, α-synuclein levels decreased to 1439 ng/ml with 5 mg/kg and 888 ng/ml with 1 mg/kg nilotinib for 6 weeks, suggesting that the decrease in brain levels may also decrease blood α-synuclein.

Because nilotinib was reported to alter autophagy (42), several autophagic markers were examined to determine whether autophagy facilitates the clearance of brain α-synuclein. Daily i.p. injection of 10 mg/kg nilotinib for 3 weeks into 7–8-month-old A53T mice decreased monomeric (41%) and high molecular weight human α-synuclein (Fig. 2E

Downloaded from https://academic.oup.com/hmg/article/22/16/3315/627350 by guest on 21 August 2022

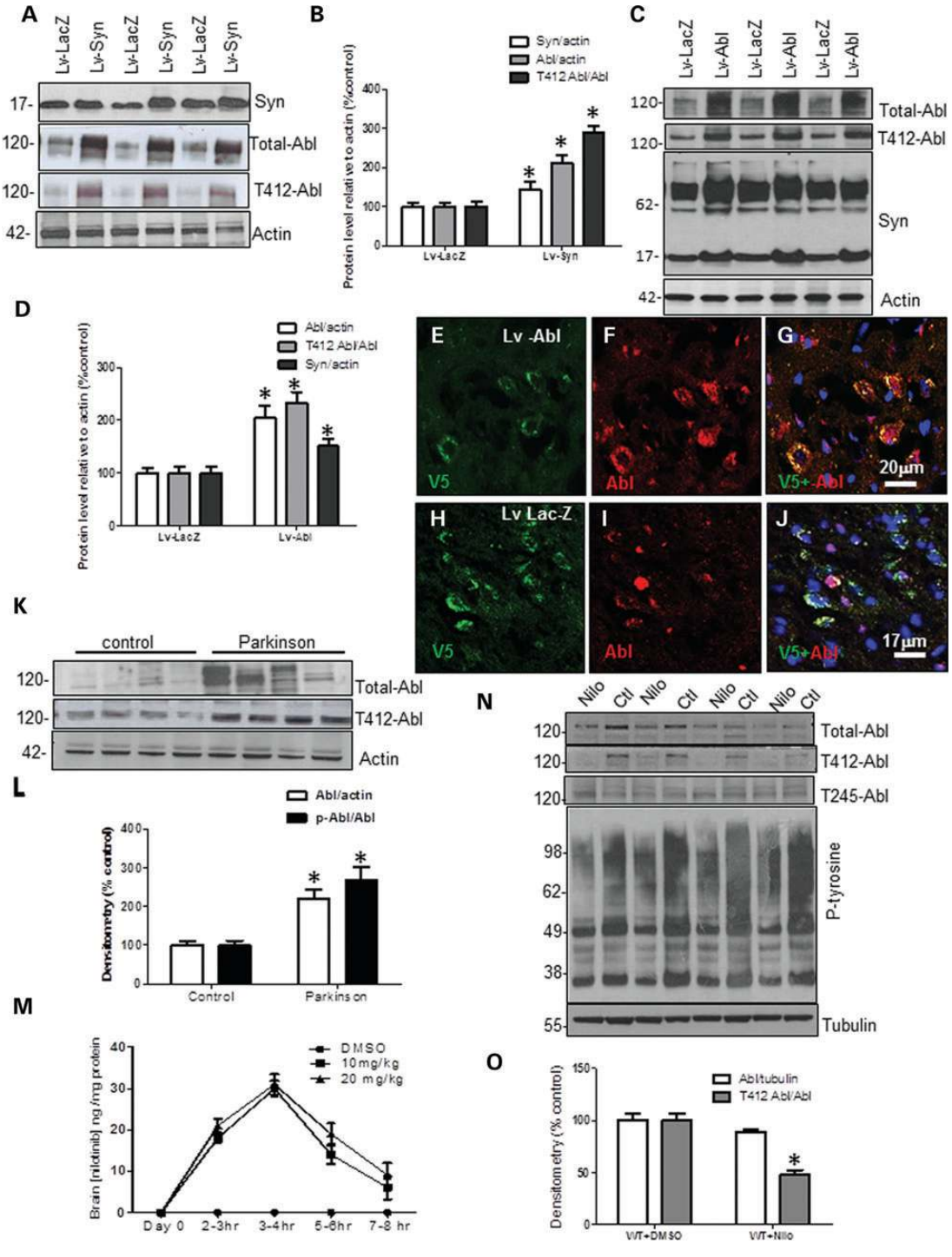

Figure 1. Abl activation is associated with accumulation of α-synuclein. WB on 10% SDS-NuPAGE gel shows (**A**) lentiviral α-synuclein expression (first blot), total Abl (second blot) and tyrosine 412 (T412) phosphorylated Abl (third blot) relative to actin ($n = 9$) and (**B**) graphs represent densitometry analysis. (**C**) Total Abl (first blot) and tyrosine 412 (T412) phosphorylated Abl (second blot), and mouse α-synuclein expression (third blot) relative to actin ($n = 9$) in lentiviral Abl- and LacZ-injected mice, and (**D**) graphs represent densitometry analysis. IHC in 20 μm thick brain sections showing (**E**) V5, (**F**) Abl and (**G**) merged V5 and Abl staining in the SN of mice injected with lentiviral Abl. IHC in 20 μm thick brain sections showing (**H**) V5, (**I**) Abl and (**J**) merged V5 and Abl staining in the SN of mice injected with lentiviral LacZ. WB on 4–12% SDS-NuPAGE gel shows (**K**) total Abl (first blot) and T412 Abl (second blot) relative to actin in human post-mortem striatal extracts, $n = 9$ PD and 7 controls, $P < 0.02$, two-tailed t-test, and (**L**) densitometry of human WBs. (**M**) Graph represents quantification of mass spectroscopy analysis of brain nilotinib ($n = 5$/time point). (**N**) WB on 4–12% SDS-NuPAGE gel shows total Abl (first blot), T412 Abl (second blot) T245 Abl (third blot) and phosphotyrosine (fourth blot) relative to parkin in wild-type mice injected with DMSO or nilotinib once daily for 3 weeks and (**O**) graphs represent densitometry analysis. *Significantly different, ANOVA, Neumann–Keuls multiple comparison, $P < 0.05$. n = number of animals, and bars are means.

Downloaded from https://academic.oup.com/hmg/article/22/16/3315/627350 by guest on 21 August 2022

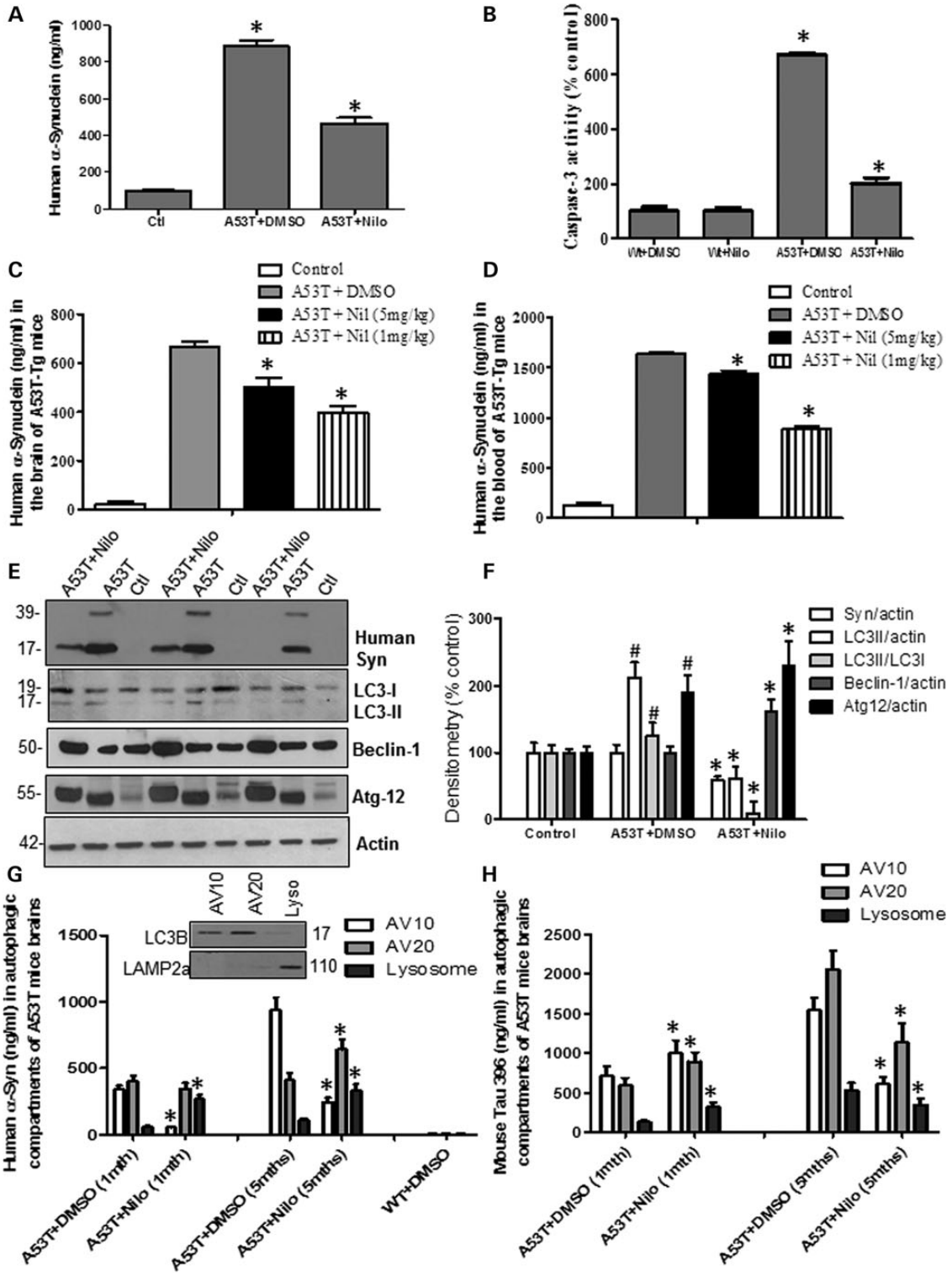

Figure 2. Abl inhibition via nilotinib promotes autophagic degradation of α-synuclein. Graphs represent ELISA measurement of (**A**) human α-synuclein ($n = 14$) and (**B**) caspase-3 activity ($n = 64$) in 6–8-month-old transgenic A53T mice and wild-type age-matched controls injected daily i.p. with 10 mg/kg nilotinib for 3 weeks. Graphs represent ELISA measurement of (A) brain levels of human α-synuclein ($n = 10$) and (B) blood levels of human α-synuclein ($n = 10$) in 5-month-old transgenic A53T mice and wild-type age-matched controls treated i.p. with 5 mg/kg or 1 mg/kg nilotinib every other day for 6 weeks. WB analysis on 4–12% SDS-NuPAGE gel shows (**E**) monomeric and high molecular weight human α-synuclein (first blot), LC3 (second blot), Beclin-1 (third blot) and Atg12 (fourth blot) relative to actin ($n = 9$) in A53T mice treated daily i.p. with 10 mg/kg nilotinib for 3 weeks, and (**F**) densitometry analysis. Graphs represent ELISA measurement of (**G**) human α-synuclein (insert shows WB of AVs) and (**H**) p-Tau levels in A53T mice ($n = 5$) treated daily i.p. with 10 mg/kg nilotinib for 3 weeks. *Significantly different, ANOVA, Neumann–Keuls multiple comparison, $P < 0.05$. n = number of animals, bars are means.

Downloaded from https://academic.oup.com/hmg/article/22/16/3315/627350 by guest on 21 August 2022

and F, $P < 0.05$, $n = 9$) relative to actin compared with A53T mice treated with DMSO. A significant increase (212%) in light chain-3 (LC3)-II (which indicates the amount of autophagosomes) relative to actin was observed in A53T mice treated with DMSO compared with wild-type (Fig. 2E and F), while LC3-II levels were decreased to 61% of control level in nilotinib-treated mice (Fig. 2E and F, $P < 0.05$, $n = 9$). A significant increase (126%) in LC3-II relative to LC3-I was also observed in A53T mice treated with DMSO compared with wild-type (Fig. 2E and F), while LC3-II/LC3-I levels were decreased to 9% of control level in nilotinib-treated mice (Fig. 2E and F, $P < 0.05$, $n = 9$). No differences in Beclin-1 levels were observed between A53T treated with DMSO and wild-type control, but nilotinib significantly increased Beclin-1 to 62% above control level (Fig. 2E and F, $P < 0.05$, $n = 9$). A significant increase in Atg12 (190%) relative to actin was detected in A53T mice treated with DMSO compared with control, but nilotinib further increased Atg-12 to 231% above control relative to actin (Fig. 2E and F, $P < 0.05$, $n = 9$), indicating possible involvement of autophagic clearance of α-synuclein. To ascertain that autophagy is involved in nilotinib-mediated α-synuclein clearance in A53T mice *in vivo*, AVs were isolated via subcellular fractionation using a discontinuous metrizamide gradient (43) and the levels of α-synuclein and hyper-phosphorylated Tau (p-Tau) were measured via ELISA. Subcellular fractionation was performed in an age-dependent manner to determine whether higher levels of protein accumulation alter autophagic flux through the AV10 or AV20 metrizamide gradients, which contain LC3B (Fig. 2G, inset), indicating phagophore/autophagosome presence and the lysosomal fraction containing lysosomal associated membrane protein (LAMP)-2a. Human α-synuclein was detected in AV10 (340 ng/ml) and AV20 (401 ng/ml) in 1-month-old A53T brains (Fig. 2G, $P < 0.05$, $n = 5$), but 10 mg/kg nilotinib significantly decreased α-synuclein levels (56 ng/ml) in AV10 (Fig. 1G, $P < 0.05$, $n = 5$). However, nilotinib significantly increased α-synuclein levels in the lysosomes (268 ng/ml) compared with DMSO (59 ng/ml). α-Synuclein was even higher in AV10 (940 ng/ml) and AV20 (410 ng/ml) in 5-month-old A53T mice treated with DMSO (Fig. 2G, $P < 0.05$, $n = 5$), but α-synuclein levels were decreased by nilotinib in AV10 (245 ng/ml) and increased in AV20 (642 ng/ml) compared with DMSO. Nilotinib also significantly increased α-synuclein levels in the lysosomes (333 ng/ml) compared with DMSO (109 ng/ml) in the same age group. p-Tau was also used as another protein marker that can potentially be degraded by autophagy. p-Tau was detected in AV10 (710 ng/ml), AV20 (590 ng/ml) and lysosomes (129 ng/ml) in 1-month-old A53T mouse brain (Fig. 2H, $P < 0.05$, $n = 5$), indicating Tau hyper-phosphorylation. However, 10 mg/kg nilotinib increased p-Tau in AV10 (1001 ng/ml), AV20 (890 ng/ml) and lysosomes (321 ng/ml) compared with DMSO within the same age group (Fig. 2H, $P < 0.05$, $n = 5$). p-Tau was even higher in AV10 (1540 ng/ml) and AV20 (2055 ng/ml) in 5-month-old A53T mice treated with DMSO (Fig. 2G, $P < 0.05$, $n = 5$), but nilotinib decreased p-Tau in AV10 (610 ng/ml) and increased it in AV20 (1133 ng/ml) compared with DMSO. Nilotinib also significantly decreased p-Tau levels in the lysosomes (345 ng/ml) compared with DMSO (530 ng/ml) in the same age group, indicating p-Tau clearance via autophagy.

Nilotinib attenuates α-synuclein levels in A53T mice

To verify the effects of nilotinib on the level of human α-synuclein in the A53T brain (6–8 months old), IHC was performed on 20 μm thick brain sections and the ventral surface of the mesencephalon was oriented towards the bottom of the page as indicated in Figure 3A. Low magnification images showed no loss of tyrosine hydroxylase (TH) neurons in the ventral tegmental area (VTA) and the SN (Fig. 3B) in A53T mice, consistent with previous reports stating no α-synuclein expression in the SN or loss of TH neurons in A53T mice (39). IHC showed abundant expression of human α-synuclein in the striatum of 6–8-month-old transgenic A53T mice treated with DMSO (Fig. 3C), cortex (Fig. 3E) and hippocampus (Fig. 3G). Daily i.p. injection of 10 mg/kg nilotinib for 3 weeks led to a decrease (72% by stereology) of human α-synuclein in the striatum (Fig. 3D), and reduced cortical (Fig. 3F, 71% by stereology) and hippocampal (Fig. 3H, 81% by stereology) α-synuclein ($P < 0.05$, $n = 7$) in transgenic A53T mice.

Abl inhibition via nilotinib promotes autophagic degradation of α-synuclein

To determine the effects of nilotinib on TH neurons, 6-month-old male C57BL/6 mice were stereotaxically injected with 1×10^4 m.o.i. lentiviral human wild-type α-synuclein (or LacZ) bilaterally into the SN for 3 weeks, and then half were treated daily with i.p. injection of 10 mg/kg nilotinib and the other half with DMSO (30 μl) for three additional weeks. ELISA measurement of SN lysates showed that human α-synuclein levels peaked at 202 ng/ml in lentiviral α-synuclein mice treated with DMSO, and nilotinib significantly reversed this increase to 31 ng/ml compared with LacZ with and without nilotinib (Fig. 4A, $P < 0.05$, $n = 9$). Daily i.p. injection of 10 mg/kg nilotinib or DMSO (30 μl) for 3 weeks did not result in any difference in caspase-3 activity in LacZ-injected SN mice (Fig. 4B, $n = 14$), but lentiviral α-synuclein expression (6 weeks total) increased caspase-3 activity 940% above control level (Fig. 4B, $P < 0.05$, $n = 14$) and 3-week nilotinib treatment reversed this increase to 140% (which remained significantly high) above LacZ levels ($P < 0.05$, $n = 14$). WB showed that nilotinib decreased (42%) the expression levels of monomeric α-synuclein (Fig. 4C and D, $P < 0.05$, $n = 9$) relative to actin compared with DMSO. Nilotinib significantly ($P < 0.05$) decreased the levels of LC3-II/actin (59%) and LC3-II/LC3-I (49%), suggesting autophagosome clearance; while it increased the expression levels of Beclin-1 (54%) and Atg12 (74%) relative to actin compared with DMSO (Fig. 4C and D, $P < 0.05$, $n = 9$). To ascertain that nilotinib did not affect α-synuclein mRNA level in the lentiviral model, qRT-PCR was performed using specific human α-synuclein primers that were initially used in the cloning of α-synuclein into the lentiviral plasmid. As expected, no human α-synuclein was detected in the LacZ-injected mice, but human α-synuclein mRNA was equally present relative to GADPH in both the DMSO and nilotinib-treated lentiviral injected mice (Fig. 4E and F), indicating that nilotinib decreases the level of α-synuclein.

To further determine whether autophagy mediates α-synuclein clearance, human M17 neuroblastoma cells were

Downloaded from https://academic.oup.com/hmg/article/22/16/3315/627350 by guest on 21 August 2022

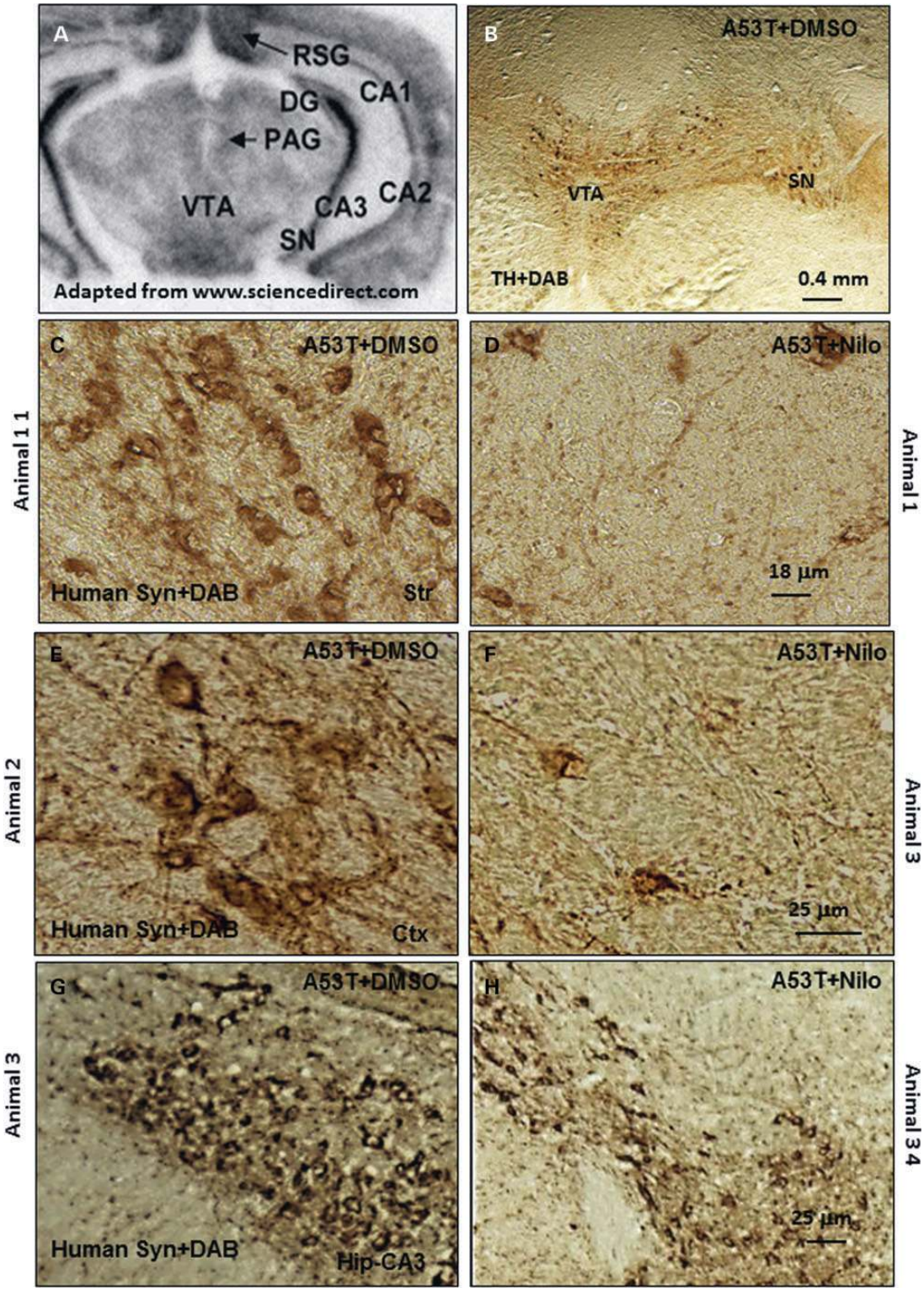

Figure 3. Nilotinib attenuates α-synuclein levels in A53T mice. (**A**) An MRI scan of a mouse brain showing brain orientation in subsequent images. Immunohistochemical staining of 20 μm thick brain sections shows (**B**) no loss of TH in VTA and SN in 6–8-month-old A53T mice, and abundant expression of human α-synuclein in (**C**) the striatum of DMSO-treated A53T mice, and (**D**) striatum of nilotinib-treated A53T mice, (**E**) the cortex of DMSO-treated A53T mice, (**F**) cortex of nilotinib-treated A53T mice, (**G**) the hippocampus of DMSO-treated A53T mice, and (**H**) hippocampus of nilotinib-treated A53T mice. The images represent different animals with daily i.p. injection of nilotinib for 3 weeks.

Downloaded from https://academic.oup.com/hmg/article/22/16/3315/627350 by guest on 21 August 2022

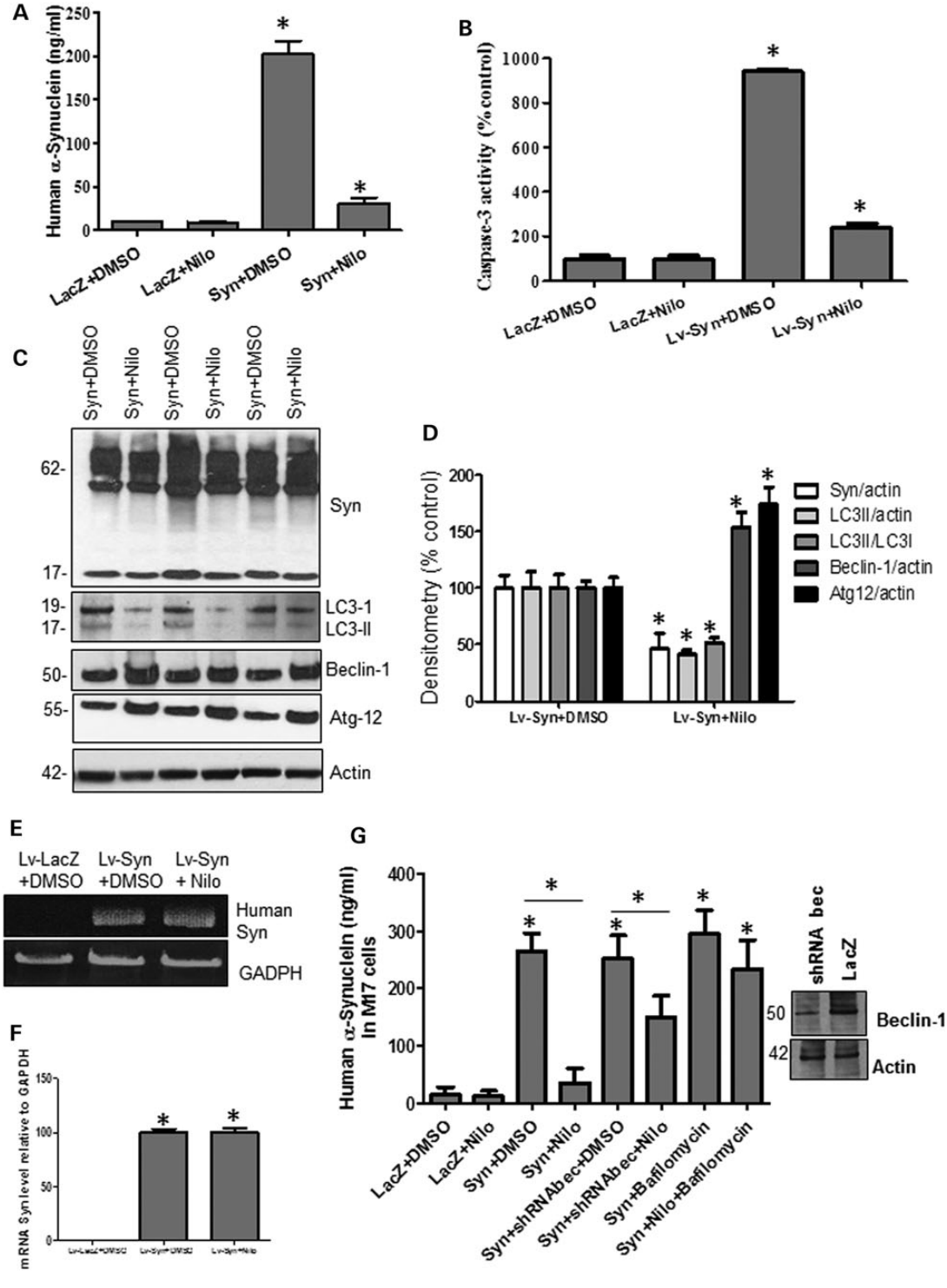

Figure 4. Nilotinib attenuates α-synuclein levels in the SN of gene transfer mice. Graphs represent ELISA measurement in mesencephalic extracts showing (**A**) human α-synuclein ($n = 9$) and (**B**) caspase-3 activity ($n = 14$) in 6-month-old C57BL/6 mice injected with lentiviral α-synuclein or LacZ into the SN for 3 weeks and treated daily i.p. with 10 mg/kg nilotinib for three additional weeks. WB analysis on 4–12% SDS-NuPAGE gel shows (**C**) monomeric and high molecular weight mouse α-synuclein (first blot), LC3 (second blot), Beclin-1 (third blot) and Atg12 (fourth blot) relative to actin ($n = 9$) in 6-month-old C57BL/6 mice injected with lentiviral α-synuclein or LacZ into the SN for 3 weeks and treated daily i.p. with 10 mg/kg nilotinib for three additional weeks, and (**D**) densitometry analysis. (**E**) Gels represent the levels of human α-synuclein mRNA in 6-month-old C57BL/6 mice injected with lentiviral α-synuclein or LacZ into the SN for 3 weeks and treated daily i.p. with 10 mg/kg nilotinib for three additional weeks and (**F**) graphs represent quantification of RT-PCR results relative to GADPH. (**G**) ELISA of human α-synuclein in M17 neuroblastoma cells transfected with 3 μg LacZ, α-synuclein cDNA or Beclin-1 shRNA for 24 h and then treated with 10 μM nilotinib for additional 24 h with and without bafilomycin A1 ($n = 12$). *Significantly different, ANOVA, Neumann–Keuls multiple comparison, $P < 0.05$. n = number of animals or number of cell culture experiments. Bars are means.

Downloaded from https://academic.oup.com/hmg/article/22/16/3315/627350 by guest on 21 August 2022

transfected with 3 μg LacZ, α-synuclein or shRNA Beclin-1 for 24 h and then treated with 10 μM nilotinib for additional 24 h. Some cells were also treated with 100 nM bafilomycin A1 for 3 h before harvest to block autophagy via impairment of autophagosome fusion with the lysosome (44). ELISA measurement showed an increase in α-synuclein (264 ng/ml) in α-synuclein transfected cells compared with LacZ (Fig. 4G, $P < 0.05$, $n = 12$) treated with 1 μl DMSO. However, nilotinib reversed α-synuclein level to 35 ng/ml ($P < 0.05$) but blocking Beclin-1 expression with shRNA (Fig. 4G, insert shows reduction of Beclin-1 expression) attenuated nilotinib-mediated clearance of α-synuclein (150 ng/ml) compared with DMSO (251 ng/ml), suggesting autophagic involvement in α-synuclein clearance. Blocking autophagy with 100 nM bafilomycin (Fig. 4G, $n = 12$) resulted in nilotinib failure to clear α-synuclein (233 ng/ml), which remained significantly higher than α-synuclein transfection with nilotinib. Taken together, these data indicate nilotinib-induced α-synuclein clearance via autophagy.

Nilotinib protects SN TH neurons from α-synuclein toxicity

IHC of 20 μm thick brain sections showed human α-synuclein expression in mice injected with lentiviral α-synuclein into the SN and treated with DMSO (Fig. 5B) compared with LacZ treated with nilotinib (or DMSO data not shown) mice (Fig. 5A, $n = 12$); but nilotinib led to 84% (by stereology) decrease of human α-synuclein (Fig. 5C, $P < 0.05$, $n = 12$) in SN neurons. A significant decrease in TH^+ neurons (89% by stereology) was observed in lentiviral α-synuclein treated with DMSO (Fig. 5E and H) compared with LacZ treated with nilotinib (Fig. 5D and G) mice, and nilotinib treatment of α-synuclein expressing mice reversed TH^+ neuron loss back to 82% (Fig. 5F and I, by stereology) of LacZ level ($P < 0.05, n = 12$). Stereological counting also showed a decrease (72%) in TH^+ (Fig. 5K) and Nissl-stained (5N) neurons in lentiviral α-synuclein treated with DMSO compared with LacZ treated with nilotinib (Fig. 5J and M). However, nilotinib attenuated (64% by stereology) loss of TH^+ (Fig. 5L) and Nissl-stained (Fig. 5O) neurons in lentiviral α-synuclein compared with DMSO-treated mice ($P < 0.05, n = 12$), suggesting that α-synuclein causes cell death and not down-regulation of TH.

Nilotinib clears cytosolic debris in SN neurons, increases DA level and improves motor performance

Transmission electron microscopy showed accumulation of cytosolic debris (Fig. 6A) and AVs in the SN of lentiviral α-synuclein expressing mice treated with DMSO (Fig. 6A, C and E). Accumulation of cytosolic AVs containing debris was consistently observed in lentiviral α-synuclein expressing mice (Fig. 6C and E), suggesting autophagosome accumulation. However, nilotinib treatment reduced accumulation of cytosolic debris and led to appearance of larger AVs at different levels of maturation (Fig. 6B, D and F) and these AVs seemed to be derived from fusion of multiple autophagic compartments, suggesting autophagic clearance.

To evaluate α-synuclein and nilotinib effects on DA metabolism, DA and its metabolite homovanilic acid (HVA) in SN brain extracts were measured using ELISA. A significant decrease ($P < 0.05$, $n = 8$) in DA (62%) and HVA (36%) was observed in SN extracts of lentiviral α-synuclein treated with DMSO compared with LacZ mice with and without nilotinib (Fig. 6G). However, nilotinib injection significantly ($P < 0.05$, $n = 8$) reversed DA and HVA loss back to control LacZ levels (Fig. 6G, $n = 8$). Lentiviral α-synuclein expression in SN decreased rotarod motor performance 39% (Fig. 6B, $P < 0.05$, $n = 14$) of LacZ controls with and without nilotinib, but nilotinib treatment of α-synuclein mice reversed motor performance to 86% of LacZ level (Fig. 6G, $P < 0.05$, $n = 14$), suggesting that reversal of DA levels leads to improved motor performance.

DISCUSSION

These studies identified Abl inhibition via nilotinib as a potential therapeutic target to treat PD and other α-synucleinopathies. Abl activation is observed in neurodegeneration (14–17), including Parkinsonism (19). Our results show that an increase in α-synuclein expression promotes Abl activity (via phosphorylation), and conversely, Abl expression increases α-synuclein accumulation in PD animal models, in agreement with the increase in Abl levels in post-mortem striatum of PD patients. Nilotinib is a non-specific TKI, which inhibits Abl phosphorylation at T412 but also reduces the level of tyrosine phosphorylated proteins in young wild-type mice, perhaps accounting to the observed decrease in total Abl after chronic treatment. The decrease in α-synuclein levels with both 1 and 5 mg/kg nilotinib suggests that possible non-specific pleotropic effects on other tyrosine kinases using higher doses of nilotinib (10 and 5 mg/kg) do not interfere with its ability to clear α-synuclein with a lower (1 mg/kg) concentration. These data indicate that a low dose of nilotinib may stimulate autophagic clearance of α-synuclein, despite the short time (up to 8 h) of nilotinib presence in the brain, suggesting that nilotinib turns autophagic clearance on to degrade α-synuclein that has accumulated in the cells between different treatments. The low dose of nilotinib may be beneficial because it may degrade α-synuclein via autophagy over a longer time without triggering self-cannibalization, which may cause cell death. The decrease in blood as well as brain α-synuclein in A53T mice indicates that degradation of brain α-synuclein reduces its blood levels, suggesting that α-synuclein may be secreted from the brain to the blood (45–49). Although A53T mice express abundant α-synuclein under the control of a prion promoter in the brain and peripheral tissues (39), the observed decrease in α-synuclein in AVs suggest that brain α-synuclein is degraded via autophagy, leading to decreased α-synuclein secretion from neurons and into the blood (45–49). α-Synuclein induces autophagic defects in the mouse brain, leading to accumulation of AVs and decreased clearance as suggested by increased LC3-II levels. Recent reports suggested that α-synuclein aggregation in A53T mice is associated with defects in chaperone-mediated autophagy, leading to cell death (50), and others reported that α-synuclein aggregation inhibits autophagy (34,35). We previously showed that lentiviral expression of α-synuclein in the rat striatum impairs autophagy (33). However, boosting autophagy with nilotinib leads to disappearance of LC3-II along with an increase in key autophagy marker, Beclin-1, suggesting that α-synuclein clearance is mediated via the Beclin-1 pathway. Lentiviral delivery to express Beclin-1 activates autophagy and improves

Downloaded from https://academic.oup.com/hmg/article/22/16/3315/627350 by guest on 21 August 2022

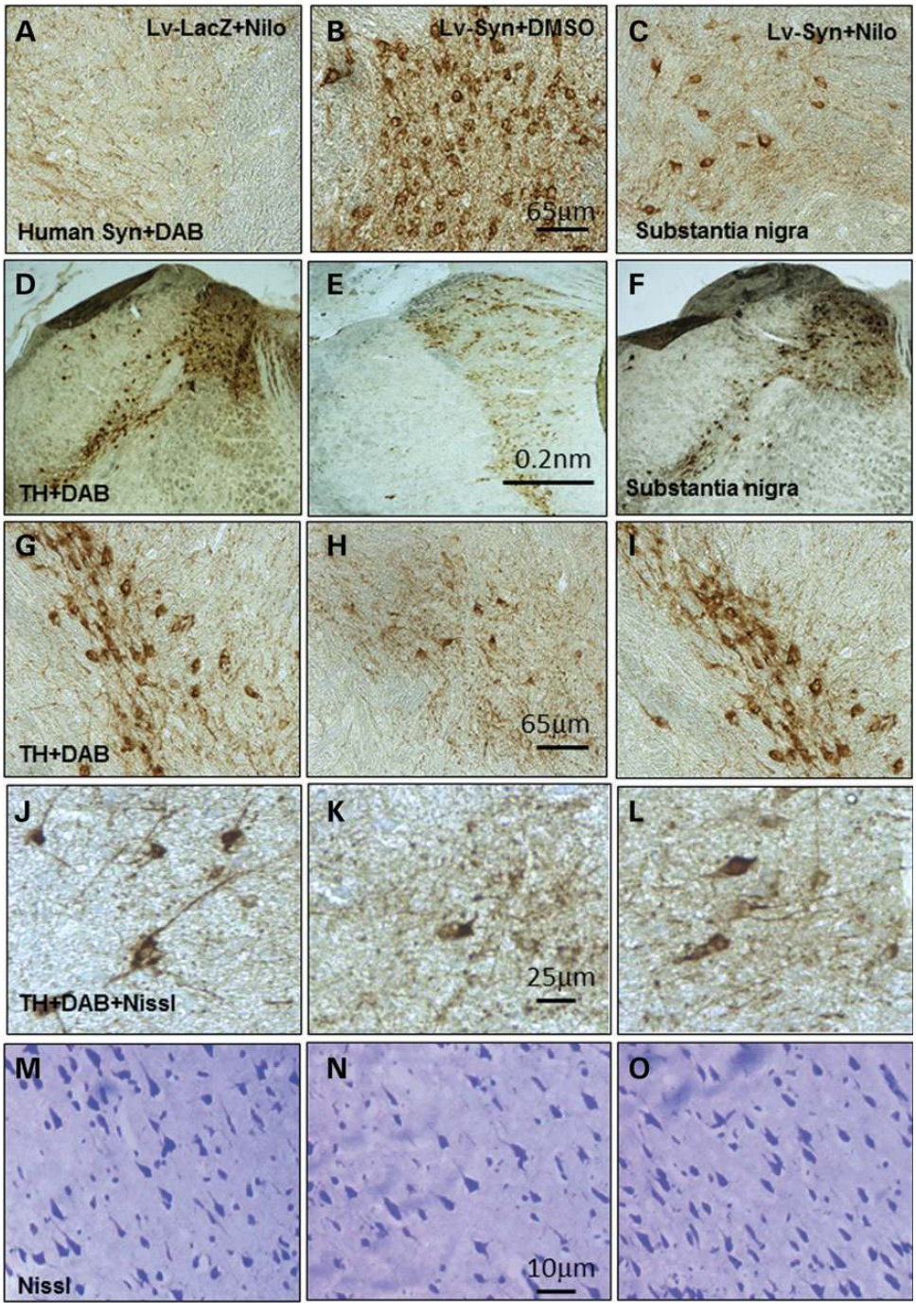

Figure 5. Nilotinib clears α-synuclein and protects TH^+ neurons. Immunohistochemical staining of 20 μm thick brain sections shows human α-synuclein in the SN of (**A**) lentiviral LacZ injected mice treated with 10 mg/kg nilotinib, (**B**) lentiviral α-synuclein treated with DMSO and (**C**) lentiviral α-synuclein treated with 10 mg/kg nilotinib daily for 3 weeks. Immunohistochemical staining of 20 μm thick brain sections show TH in (**D**) lentiviral LacZ injected with nilotinib, and (**G**) is higher magnification from a different animal, (**E**) lentiviral α-synuclein and treated with DMSO, and (**H**) is higher magnification from a different animal. (**F**) Lentiviral α-synuclein treated with nilotinib, and (**I**) is higher magnification from a different animal. High magnification of (**J**) TH^+ neurons and (**M**) Nissl-stained sections in lentiviral LacZ treated with DMSO. High magnification of (**K**) TH^+ neurons and (**N**) Nissl-stained sections in lentiviral α-synuclein treated with DMSO. High magnification of (**L**) TH^+ neurons and (**O**) Nissl-stained sections in lentiviral α-synuclein treated with 10 mg/kg nilotinib for 3 weeks.

neurodegenerative pathology in α-synuclein PD models (51). The current data showed that decreased Beclin-1 expression with shRNA compromises nilotinib ability to clear α-synuclein, in a similar manner to bafilomycin A1 treatment, raising the possibility that increased Beclin-1 levels may facilitate autophagosome maturation and subsequent AVs delivery to lysosomes for protein degradation (52). These studies show that lentiviral delivery of α-synuclein can induce autophagic changes in a relatively fast manner compared with existing transgenic mice and can mimic PD-like degeneration of SN DA

Downloaded from https://academic.oup.com/hmg/article/22/16/3315/627350 by guest on 21 August 2022

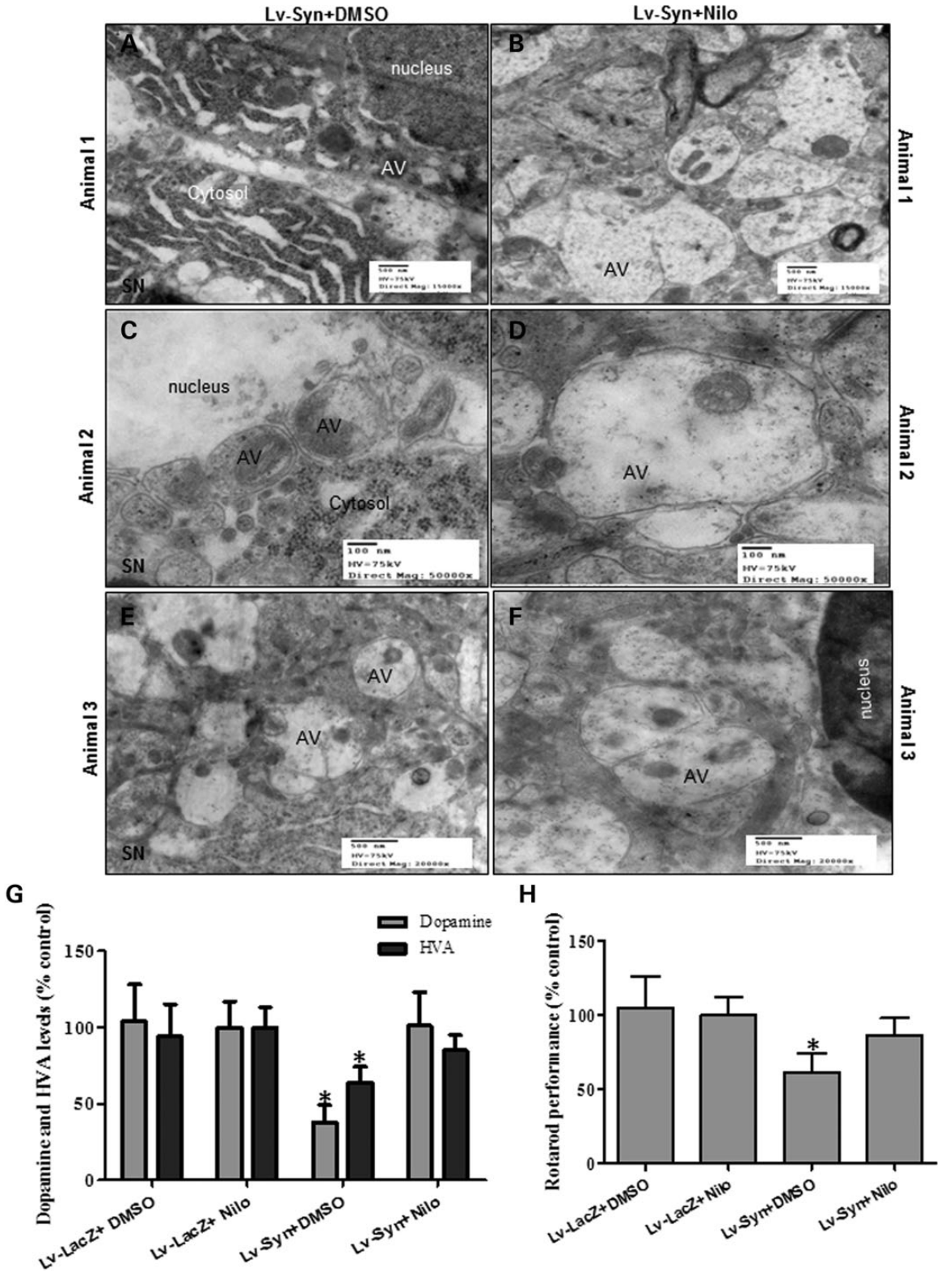

Figure 6. Nilotinib clears AVs, increases DA level and improves motor performance in SN of lentiviral α-synuclein mice. Transmission electron microscopy of SN neurons shows (**A**, **C**, **E**) accumulation of cytosolic debris and AVs in lentiviral α-synuclein expressing mice treated with DMSO. (**B**, **D**, **F**) Appearance of larger AVs with different levels of maturation in lentiviral α-synuclein treated with 10 mg/kg nilotinib for 3 weeks. Graphs represent (**G**) DA and HVA ELISA levels in mesencephalon brain extracts of lentiviral α-synuclein treated with DMSO compared with LacZ mice ($n = 8$) and (**H**) shows time spent (%) on rotarod in lentiviral α-synuclein or LacZ injected mice with and without nilotinib ($n = 14$). *Significantly different, ANOVA, Neumann–Keuls multiple comparison, $P < 0.05$. $n =$ number of animals, bars are means.

Downloaded from https://academic.oup.com/hmg/article/22/16/3315/627350 by guest on 21 August 2022

neurons and motor impairment (1–3). Several transgenic animal models show that α-synuclein expression causes death of TH^+ neurons in SN (53–57). Nilotinib treatment led to autophagic clearance of α-synuclein, decreased caspase-3 activity and prevented loss of TH^+ neurons in lentiviral α-synuclein models. Nilotinib reversed a loss of DA in α-synuclein expressing SN neurons, leading to improvement of motor performance.

Nilotinib is an FDA-approved drug and is used at 50–1200 mg/day in human patients (36). We observe biological effects, including Abl inhibition and autophagic clearance of α-synuclein at 10 mg/kg *in vivo*, indicating a dose (1000 mg/100 kg) within the clinically used range. Nilotinib administration is fairly tolerated in human CML patients but with a number of side effects, including gastrointestinal complications, vomiting and nausea and sometimes dizziness (36). Homozygous Abl mutant mice display dramatically enlarged hearts due to abnormally increased cardiomyocyte proliferation during later stages of embryogenesis (58). Disruption of Abl in mice results in neonatal lethality accompanied by pleiotropic developmental defects with variable penetrance, including runting, splenic and thymic atrophy, B cell lymphopenia, dysfunctional osteoblasts and foreshortened crania (59–61). Although Abl has an essential role in mammalian development, adult complications with Abl inhibition include edema, nausea/vomiting, muscle cramps, neutropenia, thrombocytopenia, fever, liver toxicity, arthralgia and exanthema/rash (62). Therefore, clinical use of Abl inhibition may have dose-limiting toxicity, but it may be used at low doses in neurodegeneration, due to the slow and progressive nature of neurodegenerative diseases. Although nilotinib is washed out of the brain within several hours, its effects do not seem to be limited to Abl inhibition. Lower dose and prolonged period of nilotinib administration also led to decreased α-synuclein levels, perhaps due to chronic drug treatment and potential multiple effects on several tyrosine kinases.

No drug treatment is effective as a LB disease therapy, and despite the pleiotropic effects of nilotinib, its benefits may outweigh the debilitating effects of protein accumulation in α-synucleinopathies. The current results also show age-dependent increases in p-Tau in the brain of A53T mice and nilotinib treatment can reduce p-Tau levels. The efficiency of simultaneous autophagic degradation of both p-Tau and α-synuclein in the brain suggests that nilotinib may be an effective therapy for dementia and Parkinsonism, where both p-Tau and α-synuclein may pathologically accumulate. Nilotinib accelerates clearance of accumulating proteins and protects DA neurons, ameliorating motor performance in PD models. Therefore, the next step will be to conduct phase II clinical trials to evaluate nilotinib effects on motor performance in PD and other patients with α-synucleinopathies, including MSA and PSP.

MATERIALS AND METHODS

Stereotaxic injection

Six months old male C57BL/6 mice were stereotaxically injected with lentiviral Abl, α-synuclein (or LacZ control) bilaterally into the SN using co-ordinates: lateral: 1.5 mm, ventral: 4.1 mm and horizontal: −3.64. The lentivirus was tittered in human M17 neuroblastoma cells according to the Invitrogen protocol. Titration and lentiviral expression was verified via counting the V5 tag-positive cells as virally infected cells relative to the total number of cells in 12-well dishes (Falcon). The number of viral genomes was calculated and a total number of 1×10^4 viral particles were injected into the mouse SN in a total of 6 μl. Viral stocks were injected through a microsyringe pump controller (Micro4) using total pump (World Precision Instruments, Inc.) delivery of 2 μl at a rate of 0.2 μl/min as previously described (63–65). All animal experiments were conducted in full compliance with the recommendations of Georgetown University Animal Care and Use Committee (GUAUC). *n* is the number of animals in each experiments, and all data are expressed as means.

Nilotinib treatment

Three weeks post-injection with the lentivirus, half the animals were i.p. treated daily with 10 mg/kg nilotinib dissolved in DMSO and the other half received DMSO treatments (3 μl total) for an additional 3 weeks. Half of A53T transgenic mice were i.p. treated daily with 10 mg/kg nilotinib and the other half with DMSO. Lower dose of nilotinib including 1 and 5 mg/kg were administered i.p. every other day for 6 weeks.

WB analysis

The nigrostriatal region was isolated from α-synuclein or Abl expressing mice and compared with LacZ or total brain extracts from A53T mice. Tissues were homogenized in 1 × Sodium Tris EDTA NP40 (STEN) lysis buffer [50 mM sodium Tris (pH 7.6), 150 mM NaCl, 2 mM EDTA, 0.2% NP-40, 0.2% BSA, 20 mM PMSF and protease cocktail inhibitor], centrifuged at 10 000*g* for 20 min at 4°C and the supernatant containing the soluble protein fraction was collected. The supernatant was analyzed by WB on SDS-NuPAGE Bis–Tris gel (Invitrogen). Mouse α-synuclein was probed with (1:1000) anti-α-Synuclein antibody (BD Transduction Laboratories, USA) and human α-synuclein was probed (1:1500) with human antibodies (ThermoScientific). Total Abl was probed with (1:500) rabbit polyclonal (K12) antibody (Thermo Fisher), or p-Abl (T412) with (1:500) rabbit polyclonal antibody (Millipore) or p-Abl (T245) with (1:500) rabbit polyclonal antibody (Millipore). Phosphotyrosine proteins were probed (1:1000) with rabbit polyclonal antibody (Cell signaling). β-Actin was probed (1:1000) with polyclonal antibody (Cell Signaling Technology, Beverly, MA, USA). Autophagy antibodies, including rabbit polyclonal Beclin-1 (1:1000) and rabbit polyclonal Atg12 (1:1000), were used according to autophagy antibody sampler kit 4445 (Cell Signaling, Inc). A rabbit polyclonal (Pierce) anti-LC3 (1:1000) and rabbit polyclonal (Thermo Scientific) anti-actin (1:1000) were used. Rabbit polyclonal (1:1000) tubulin (Thermo Scientific) was used. MAP-2 was probed (1:1000) with mouse monoclonal antibody (Pierce). WBs were quantified by densitometry using the Quantity One 4.6.3 software (Bio Rad).

IHC of brain sections

Animals were deeply anesthetized with a mixture of xylazine and ketamine (1:8), washed with 1 × saline for 1 min and then perfused with 4% paraformaldehyde (PFA) for 15–20 min.

Downloaded from https://academic.oup.com/hmg/article/22/16/3315/627350 by guest on 21 August 2022

Brains were quickly dissected out and immediately stored in 4% PFA for 24 h at 4°C, and then transferred to 30% sucrose at 4°C for 48 h. TH was probed (1:100) with rabbit polyclonal (AB152) antibody (Millipore) and human α-synuclein was probed (1:100) with mouse monoclonal antibodies (Thermo Scientific) and DAB counterstained. Abl was probed (1:100) with (K12) rabbit polyclonal antibody (Thermo Fisher), and V5 was probed (1:500) with an epitope tag rabbit polyclonal antibody (Thermo Scientific). Nissl staining was performed according to the manufacturer's protocols (Sigma Aldrich).

Stereological methods

Stereological methods were applied by a blinded investigator using unbiased stereology analysis (Stereologer, Systems Planning and Analysis, Chester, MD, USA) to determine the total positive cell counts in 20 cortical fields on at least 10 brain sections (∼400 positive cells per animal) from each animal as previously explained (66).

Cell culture and transfection

Human neuroblastoma M17 cells were grown in 24-well dishes (Falcon) as previously described (43,67). Transient transfection was performed with 3 μg α-synuclein, or Abl cDNA or Beclin-1 shRNA (Open Biosystems), or 3 μg LacZ cDNA for 24 h. Cells were treated with 10 μM nilotinib for 24 h and/or 100 nM bafilomycin for 3 h. Cells were harvested 48 h after transfection in 1 × STEN buffer and centrifuged at 10 000*g* for 20 min at 4°C, and the supernatant was collected.

Human α-synuclein and p-Tau ELISA

Human α-synuclein and p-Tau ELISA were performed using 50 μl (1 μg/μl) of brain lysates (in STEN buffer) detected with 50 μl primary antibody (3 h) and 100 μl anti-rabbit secondary antibody (30 min) at RT. α-Synuclein levels were measured using human-specific ELISA (Invitrogen) according to the manufacturers' protocols. *p-Tau* was measured using specific p-Tau at serine 396 according to the manufacturer's protocol as previously described (43,67).

Caspase-3 fluorometric activity assay

To measure caspase-3 activity in the animal models, we used EnzChek® caspase-3 assay kit #1 (Invitrogen) on cortical extracts and Z-DEVD-AMC substrate and the absorbance was read according to the manufacturer's protocol.

ELISA dopamine and HVA

Total brain or mesencephalon was collected and fresh 50 μl (1 μg/μl) brain lysates (in STEN buffer) were detected with 50 μl primary antibody (1 h) and 100 μl anti-rabbit secondary antibody (30 min) at RT according to the manufacturer's protocols (Abnova, Cat# BOLD01090J00011) for DA and (Eagle Biosciences, Cat# HVA34-K01) for HVA.

Transmission EM

Brain tissues were fixed in (1:4, v:v) 4% PFA-picric acid solution and 25% glutaraldehyde overnight, and then washed three times in 0.1 M cacodylate buffer and osmicated in 1% osmium tetroxide/1.5% potassium ferrocyanide for 3 h, followed by another three times wash in distilled water. Samples were treated with 1% uranyl acetate in maleate buffer for 1 h, washed three times in maleate buffer (pH 5.2), then exposed to a graded cold ethanol series up to 100% and ending with a propylene oxide treatment. Samples were embedded in pure plastic and incubated at 60°C for 1–2 days. Blocks are sectioned on a Leica ultracut microtome at 95 nm, picked up onto 100 nm formvar-coated copper grids and analyzed using a Philips Technai Spirit transmission EM.

MALDI-TOF mass spectroscopy

Brain extracts (in DMSO) were freeze-dried and re-suspend in acetonitrile. Nilotinib quantification was carried out on a 4800 MALDI-TOF–TOF Analyzer (Applied Biosystems, CA, USA) in reflector-positive mode and then validated in MS/MS mode as previously described (63,68). Detected fragment masses were identified in SWISS-PROT databases using MASCOT.

Subcellular fractionation to isolate AVs

0.5 g of fresh animal brains were homogenized at low speed (Cole-Palmer homogenizer, LabGen 7, 115 Vac) in 1xSTEN buffer and centrifuged at 1000*g* for 10 min to isolate the supernatant from the pellet. The pellet was re-suspended in 1xSTEN buffer and centrifuged once to increase the recovery of lysosomes. The pooled supernatants were then centrifuged at 100 000 rpm for 1 h at 4°C to extract the pellet containing AVs and lysosomes. The pellet was then re-suspended in 10 ml (0.33 g/ml) 50% metrizamide and 10 ml in cellulose nitrate tubes. A discontinuous metrizamide gradient was constructed in layers from bottom to top as follows: 6 ml of pellet suspension, 10 ml of 26%; 5 ml of 24%; 5 ml of 20%; and 5 ml of 10% metrizamide (69). After centrifugation at 10 000 rpm for 1 h at 4°C, the fraction floating on the 10% layer (lysosome) and the fractions banding at the 24%/20% (AV 20) and the 20%/10% (AV10) metrizamide inter-phases were collected by a syringe and examined by ELISA.

Rotarod tests

Mice were placed on an accelerating rotarod (Columbus Instruments) equipped with individual timers for each mouse. Mice were trained to stay on the rod at a constant 5 rpm rotation for at least 2 min, then the speed was gradually increased by 0.2 rpm/min and the latency to fall was measured. All values were converted to % control.

qRT-PCR in brain tissues

qRT-PCR was performed on Real-time OCR system (Applied Biosystems) with Fast SYBR-Green PCR master Mix (Applied Biosystems) in triplicate from reverse-transcribed

Downloaded from https://academic.oup.com/hmg/article/22/16/3315/627350 by guest on 21 August 2022

cDNA from mouse mesencephalon injected with lentiviral LacZ or lentiviral α-synuclein (total 6 weeks) treated with DMSO or nilotinib (total 3 weeks). Human wild-type α-synuclein 'CAC CAT GGA TGT ATT CAT GTT TCC' was used as a forward primer and 'GGC TTC AGG TTC GTA GTC TTG AT' as a reverse primer. Gene expression values were normalized using GADPH levels.

AUTHORS' CONTRIBUTION

I.L. performed IHC, lentiviral preparation and Rotarod; M.L.H. performed ELISA, rotarod and western blots and edited manuscript; C.E.-H.M. injected the animals, oversaw the studies and wrote the manuscript.

Conflict of Interest statement. C.E.-H.M. has a provisional patent application to use nilotinib as a therapeutic approach in neurodegenerative diseases. Other authors declare no conflict of interest in association with this manuscript.

FUNDING

These studies were supported by NIH (grant NIA 30378) and Georgetown University funding to C.E.-H.M. The authors would like to thank Jim Driver from the University of Montana for his support in the EM studies.

REFERENCES

1. Benner, E.J., Banerjee, R., Reynolds, A.D., Sherman, S., Pisarev, V.M., Tsiperson, V., Nemachek, C., Ciborowski, P., Przedborski, S., Mosley, R.L. *et al.*. (2008) Nitrated alpha-synuclein immunity accelerates degeneration of nigral dopaminergic neurons. *PLoS ONE*, **3**, e1376.
2. Kuhn, D.M., Francescutti-Verbeem, D.M. and Thomas, D.M. (2006) Dopamine quinones activate microglia and induce a neurotoxic gene expression profile: relationship to methamphetamine-induced nerve ending damage. *Ann. N. Y. Acad. Sci.*, **1074**, 31–41.
3. Reynolds, A.D., Kadiu, I., Garg, S.K., Glanzer, J.G., Nordgren, T., Ciborowski, P., Banerjee, R. and Gendelman, H.E. (2008) Nitrated alpha-synuclein and microglial neuroregulatory activities. *J. Neuroimmune Pharmacol.*, **3**, 59–74.
4. Goedert, M. (1999) Filamentous nerve cell inclusions in neurodegenerative diseases: tauopathies and alpha-synucleinopathies. *Philos. Trans. R. Soc. Lond. B Biol. Sci.*, **354**, 1101–1118.
5. Goedert, M. (2001) Alpha-synuclein and neurodegenerative diseases. *Nat. Rev. Neurosci.*, **2**, 492–501.
6. Lundvig, D., Lindersson, E. and Jensen, P.H. (2005) Pathogenic effects of alpha-synuclein aggregation. *Brain. Res. Mol. Brain Res.*, **134**, 3–17.
7. Spillantini, M.G., Crowther, R.A., Jakes, R., Cairns, N.J., Lantos, P.L. and Goedert, M. (1998) Filamentous alpha-synuclein inclusions link multiple system atrophy with Parkinson's disease and dementia with Lewy bodies. *Neurosci. Lett.*, **251**, 205–208.
8. Spillantini, M.G., Crowther, R.A., Jakes, R., Hasegawa, M. and Goedert, M. (1998) alpha-Synuclein in filamentous inclusions of Lewy bodies from Parkinson's disease and dementia with lewy bodies. *Proc. Natl Acad. Sci. USA*, **95**, 6469–6473.
9. Spillantini, M.G. and Goedert, M. (2000) The alpha-synucleinopathies: Parkinson's disease, dementia with Lewy bodies, and multiple system atrophy. *Ann. N. Y. Acad. Sci.*, **920**, 16–27.
10. Spillantini, M.G., Schmidt, M.L., Lee, V.M., Trojanowski, J.Q., Jakes, R. and Goedert, M. (1997) Alpha-synuclein in Lewy bodies. *Nature*, **388**, 839–840.
11. Takeda, A., Hashimoto, M., Mallory, M., Sundsumo, M., Hansen, L. and Masliah, E. (2000) C-terminal alpha-synuclein immunoreactivity in structures other than Lewy bodies in neurodegenerative disorders. *Acta Neuropathol.*, **99**, 296–304.
12. Trojanowski, J.Q. and Lee, V.M. (2003) Parkinson's disease and related alpha-synucleinopathies are brain amyloidoses. *Ann. N. Y. Acad. Sci.*, **991**, 107–110.
13. Wakabayashi, K., Matsumoto, K., Takayama, K., Yoshimoto, M. and Takahashi, H. (1997) NACP, a presynaptic protein, immunoreactivity in Lewy bodies in Parkinson's disease. *Neurosci. Lett.*, **239**, 45–48.
14. Imam, S.Z., Zhou, Q., Yamamoto, A., Valente, A.J., Ali, S.F., Bains, M., Roberts, J.L., Kahle, P.J., Clark, R.A. and Li, S. (2011) Novel regulation of parkin function through c-Abl-mediated tyrosine phosphorylation: implications for Parkinson's disease. *J. Neurosci.*, **31**, 157–163.
15. Ko, H.S., Lee, Y., Shin, J.H., Karuppagounder, S.S., Gadad, B.S., Koleske, A.J., Pletnikova, O., Troncoso, J.C., Dawson, V.L. and Dawson, T.M. (2010) Phosphorylation by the c-Abl protein tyrosine kinase inhibits parkin's ubiquitination and protective function. *Proc. Natl Acad. Sci. USA*, **107**, 16691–16696.
16. Jing, Z., Caltagarone, J. and Bowser, R. (2009) Altered subcellular distribution of c-Abl in Alzheimer's disease. *J. Alzheimers Dis.*, **17**, 409–422.
17. Tremblay, M.A., Acker, C.M. and Davies, P. (2010) Tau phosphorylated at tyrosine 394 is found in Alzheimer's disease tangles and can be a product of the Abl-related kinase, Arg. *J. Alzheimers Dis.*, **19**, 721–733.
18. Wang, J.Y. (2000) Regulation of cell death by the Abl tyrosine kinase. *Oncogene*, **19**, 5643–5650.
19. Schlatterer, S.D., Acker, C.M. and Davies, P. (2011) c-Abl in neurodegenerative disease. *J. Mol. Neurosci.*, **45**, 445–452.
20. Derkinderen, P., Scales, T.M., Hanger, D.P., Leung, K.Y., Byers, H.L., Ward, M.A., Lenz, C., Price, C., Bird, I.N., Perera, T. *et al.* (2005) Tyrosine 394 is phosphorylated in Alzheimer's paired helical filament tau and in fetal tau with c-Abl as the candidate tyrosine kinase. *J. Neurosci.*, **25**, 6584–6593.
21. Schlatterer, S.D., Tremblay, M.A., Acker, C.M. and Davies, P. (2011) Neuronal c-Abl overexpression leads to neuronal loss and neuroinflammation in the mouse forebrain. *J. Alzheimers Dis.*, **25**, 119–133.
22. Seglen, P.O. (1987) In: Glaumann, H. and Ballard, F.J. (eds.), *Lysosomes: Their Role in Protein Breakdown*. Academic Press, London, pp. 369–414.
23. de Duve, C. and Wattiaux, R. (1966) Functions of lysosomes. *Annu. Rev. Physiol.*, **28**, 435–492.
24. Dunn, W.A. Jr. (1994) Autophagy and related mechanisms of lysosome-mediated protein degradation. *Trends Cell Biol.*, **4**, 139–143.
25. Gordon, P.B. and Seglen, P.O. (1988) Prelysosomal convergence of autophagic and endocytic pathways. *Biochem. Biophys. Res. Commun.*, **151**, 40–47.
26. Boland, B., Kumar, A., Lee, S., Platt, F.M., Wegiel, J., Yu, W.H. and Nixon, R.A. (2008) Autophagy induction and autophagosome clearance in neurons: relationship to autophagic pathology in Alzheimer's disease. *J. Neurosci.*, **28**, 6926–6937.
27. Kegel, K.B., Kim, M., Sapp, E., McIntyre, C., Castano, J.G., Aronin, N. and DiFiglia, M. (2000) Huntingtin expression stimulates endosomal-lysosomal activity, endosome tubulation, and autophagy. *J. Neurosci.*, **20**, 7268–7278.
28. Nixon, R.A., Wegiel, J., Kumar, A., Yu, W.H., Peterhoff, C., Cataldo, A. and Cuervo, A.M. (2005) Extensive involvement of autophagy in Alzheimer disease: an immuno-electron microscopy study. *J. Neuropathol. Exp. Neurol.*, **64**, 113–122.
29. Ravikumar, B., Duden, R. and Rubinsztein, D.C. (2002) Aggregate-prone proteins with polyglutamine and polyalanine expansions are degraded by autophagy. *Hum. Mol. Genet.*, **11**, 1107–1117.
30. Sabatini, D.M. (2006) mTOR and cancer: insights into a complex relationship. *Nat. Rev. Cancer*, **6**, 729–734.
31. Stefanis, L., Larsen, K.E., Rideout, H.J., Sulzer, D. and Greene, L.A. (2001) Expression of A53T mutant but not wild-type alpha-synuclein in PC12 cells induces alterations of the ubiquitin-dependent degradation system, loss of dopamine release, and autophagic cell death. *J. Neurosci.*, **21**, 9549–9560.
32. Webb, J.L., Ravikumar, B., Atkins, J., Skepper, J.N. and Rubinsztein, D.C. (2003) Alpha-Synuclein is degraded by both autophagy and the proteasome. *J. Biol. Chem.*, **278**, 25009–25013.
33. Lonskaya, I., Hebron, M.L., Algarzae, N.K., Desforges, N. and Moussa, C.E. (2012) Decreased parkin solubility is associated with impairment of autophagy in the nigrostriatum of sporadic Parkinson's disease. *Neuroscience*, **232C**, 90.
34. Winslow, A.R. and Rubinsztein, D.C. (2011) The Parkinson disease protein alpha-synuclein inhibits autophagy. *Autophagy*, **7**, 429–431.

Downloaded from https://academic.oup.com/hmg/article/22/16/3315/627350 by guest on 21 August 2022

35. Winslow, A.R., Chen, C.W., Corrochano, S., Acevedo-Arozena, A., Gordon, D.E., Peden, A.A., Lichtenberg, M., Menzies, F.M., Ravikumar, B., Imarisio, S. *et al.* (2010) alpha-Synuclein impairs macroautophagy: implications for Parkinson's disease. *J. Cell Biol.*, **190**, 1023–1037.
36. Deremer, D.L., Ustun, C. and Natarajan, K. (2008) Nilotinib: a second-generation tyrosine kinase inhibitor for the treatment of chronic myelogenous leukemia. *Clin. Ther.*, **30**, 1956–1975.
37. Skorski, T. (2011) BCR-ABL1 kinase: hunting an elusive target with new weapons. *Chem. Biol.*, **18**, 1352–1353.
38. Mahon, F.X., Hayette, S., Lagarde, V., Belloc, F., Turcq, B., Nicolini, F., Belanger, C., Manley, P.W., Leroy, C., Etienne, G. *et al.* (2008) Evidence that resistance to nilotinib may be due to BCR-ABL, Pgp, or Src kinase overexpression. *Cancer Res.*, **68**, 9809–9816.
39. Giasson, B.I., Duda, J.E., Quinn, S.M., Zhang, B., Trojanowski, J.Q. and Lee, V.M. (2002) Neuronal alpha-synucleinopathy with severe movement disorder in mice expressing A53T human alpha-synuclein. *Neuron*, **34**, 521–533.
40. Alvarez, A.R., Sandoval, P.C., Leal, N.R., Castro, P.U. and Kosik, K.S. (2004) Activation of the neuronal c-Abl tyrosine kinase by amyloid-beta-peptide and reactive oxygen species. *Neurobiol. Dis.*, **17**, 326–336.
41. Cancino, G.I., Toledo, E.M., Leal, N.R., Hernandez, D.E., Yevenes, L.F., Inestrosa, N.C. and Alvarez, A.R. (2008) STI571 prevents apoptosis, tau phosphorylation and behavioural impairments induced by Alzheimer's beta-amyloid deposits. *Brain*, **131**, 2425–2442.
42. Salomoni, P. and Calabretta, B. (2009) Targeted therapies and autophagy: new insights from chronic myeloid leukemia. *Autophagy*, **5**, 1050–1051.
43. Lonskaya, I., Shekoyan, A.R., Hebron, M.L., Desforges, N., Algarzae, N.K. and Moussa, C.E. (2013) Diminished parkin solubility and co-localization with intraneuronal amyloid-beta are associated with autophagic defects in Alzheimer's disease. *J. Alzheimers Dis.*, **33**, 231–247.
44. Klionsky, D.J., Elazar, Z., Seglen, P.O. and Rubinsztein, D.C. (2008) Does bafilomycin A1 block the fusion of autophagosomes with lysosomes? *Autophagy*, **4**, 849–950.
45. Danzer, K.M., Kranich, L.R., Ruf, W.P., Cagsal-Getkin, O., Winslow, A.R., Zhu, L., Vanderburg, C.R. and McLean, P.J. (2012) Exosomal cell-to-cell transmission of alpha synuclein oligomers. *Mol. Neurodegener.*, **7**, 42.
46. Lundblad, M., Decressac, M., Mattsson, B. and Bjorklund, A. (2012) Impaired neurotransmission caused by overexpression of alpha-synuclein in nigral dopamine neurons. *Proc. Natl Acad. Sci. USA*, **109**, 3213–3219.
47. Emmanouilidou, E., Elenis, D., Papasilekas, T., Stranjalis, G., Gerozissis, K., Ioannou, P.C. and Vekrellis, K. (2011) Assessment of alpha-synuclein secretion in mouse and human brain parenchyma. *PLoS ONE*, **6**, e22225.
48. Emmanouilidou, E., Melachroinou, K., Roumeliotis, T., Garbis, S.D., Ntzouni, M., Margaritis, L.H., Stefanis, L. and Vekrellis, K. (2010) Cell-produced alpha-synuclein is secreted in a calcium-dependent manner by exosomes and impacts neuronal survival. *J. Neurosci.*, **30**, 6838–6851.
49. Lee, H.J., Patel, S. and Lee, S.J. (2005) Intravesicular localization and exocytosis of alpha-synuclein and its aggregates. *J. Neurosci.*, **25**, 6016–6024.
50. Malkus, K.A. and Ischiropoulos, H. (2012) Regional deficiencies in chaperone-mediated autophagy underlie alpha-synuclein aggregation and neurodegeneration. *Neurobiol. Dis.*, **46**, 732–744.
51. Spencer, B., Potkar, R., Trejo, M., Rockenstein, E., Patrick, C., Gindi, R., Adame, A., Wyss-Coray, T. and Masliah, E. (2009) Beclin 1 gene transfer activates autophagy and ameliorates the neurodegenerative pathology in alpha-synuclein models of Parkinson's and Lewy body diseases. *J. Neurosci.*, **29**, 13578–13588.
52. Chu, C.T. (2006) Autophagic stress in neuronal injury and disease. *J. Neuropathol. Exp. Neurol.*, **65**, 423–432.
53. Recchia, A., Rota, D., Debetto, P., Peroni, D., Guidolin, D., Negro, A., Skaper, S.D. and Giusti, P. (2008) Generation of a alpha-synuclein-based rat model of Parkinson's disease. *Neurobiol. Dis.*, **30**, 8–18.
54. Bazzu, G., Calia, G., Puggioni, G., Spissu, Y., Rocchitta, G., Debetto, P., Grigoletto, J., Zusso, M., Migheli, R., Serra, P.A. *et al.* (2010) alpha-Synuclein- and MPTP-generated rodent models of Parkinson's disease and the study of extracellular striatal dopamine dynamics: a microdialysis approach. *CNS Neurol. Disord. Drug Targets*, **9**, 482–490.
55. Thiruchelvam, M.J., Powers, J.M., Cory-Slechta, D.A. and Richfield, E.K. (2004) Risk factors for dopaminergic neuron loss in human alpha-synuclein transgenic mice. *Eur. J. Neurosci.*, **19**, 845–854.
56. McCormack, A.L., Mak, S.K., Henderson, J.M., Bumcrot, D., Farrer, M.J. and Di Monte, D.A. (2010) Alpha-synuclein suppression by targeted small interfering RNA in the primate substantia nigra. *PLoS ONE*, **5**, e12122.
57. Kirik, D., Rosenblad, C., Burger, C., Lundberg, C., Johansen, T.E., Muzyczka, N., Mandel, R.J. and Bjorklund, A. (2002) Parkinson-like neurodegeneration induced by targeted overexpression of alpha-synuclein in the nigrostriatal system. *J. Neurosci.*, **22**, 2780–2791.
58. Qiu, Z., Cang, Y. and Goff, S.P. (2010) c-Abl tyrosine kinase regulates cardiac growth and development. *Proc. Natl Acad. Sci. USA*, **107**, 1136–1141.
59. Li, B., Boast, S., de los Santos, K., Schieren, I., Quiroz, M., Teitelbaum, S.L., Tondravi, M.M. and Goff, S.P. (2000) Mice deficient in Abl are osteoporotic and have defects in osteoblast maturation. *Nat. Genet.*, **24**, 304–308.
60. Schwartzberg, P.L., Stall, A.M., Hardin, J.D., Bowdish, K.S., Humaran, T., Boast, S., Harbison, M.L., Robertson, E.J. and Goff, S.P. (1991) Mice homozygous for the ablm1 mutation show poor viability and depletion of selected B and T cell populations. *Cell*, **65**, 1165–1175.
61. Tybulewicz, V.L., Crawford, C.E., Jackson, P.K., Bronson, R.T. and Mulligan, R.C. (1991) Neonatal lethality and lymphopenia in mice with a homozygous disruption of the c-abl proto-oncogene. *Cell*, **65**, 1153–1163.
62. Kantarjian, H., Sawyers, C., Hochhaus, A., Guilhot, F., Schiffer, C., Gambacorti-Passerini, C., Niederwieser, D., Resta, D., Capdeville, R., Zoellner, U. *et al.* (2002) Hematologic and cytogenetic responses to imatinib mesylate in chronic myelogenous leukemia. *N. Engl. J. Med.*, **346**, 645–652.
63. Burns, M.P., Zhang, L., Rebeck, G.W., Querfurth, H.W. and Moussa, C.E. (2009) Parkin promotes intracellular Abeta1–42 clearance. *Hum. Mol. Genet.*, **18**, 3206–3216.
64. Herman, A.M. and Moussa, C.E. (2011) The ubiquitin ligase parkin modulates the execution of autophagy. *Autophagy*, **7**, 919–921.
65. Khandelwal, P.J., Dumanis, S.B., Feng, L.R., Maguire-Zeiss, K., Rebeck, G., Lashuel, H.A. and Moussa, C.E. (2010) Parkinson-related parkin reduces alpha-Synuclein phosphorylation in a gene transfer model. *Mol. Neurodegener.*, **5**, 47.
66. Hebron, M.L., Lonskaya, I., Sharpe, K., Weerasinghe, P.P., Algarzae, N.K., Shekoyan, A.R. and Moussa, C.E. (2013) Parkin ubiquitinates Tar-DNA binding protein-43 (TDP-43) and promotes its cytosolic accumulation via interaction with histone deacetylase 6 (HDAC6). *J. Biol. Chem.*, **288**, 4103–4115.
67. Rebeck, G.W., Hoe, H.S. and Moussa, C.E. (2010) Beta-amyloid1–42 gene transfer model exhibits intraneuronal amyloid, gliosis, tau phosphorylation, and neuronal loss. *J. Biol. Chem.*, **285**, 7440–7446.
68. Khandelwal, P.J., Herman, A.M., Hoe, H.S., Rebeck, G.W. and Moussa, C.E. (2011) Parkin mediates beclin-dependent autophagic clearance of defective mitochondria and ubiquitinated Abeta in AD models. *Hum. Mol. Genet.*, **20**, 2091–2102.
69. Marzella, L., Ahlberg, J. and Glaumann, H. (1982) Isolation of autophagic vacuoles from rat liver: morphological and biochemical characterization. *J. Cell. Biol.*, **93**, 144–154.

Downloaded from https://academic.oup.com/hmg/article/22/16/3315/627350 by guest on 21 August 2022